DOI: 10.1109/TMAG.2014.2347963

Strength Pareto Evolutionary Optimization of an In-wheel PM Motor with Unequal Teeth for Electric Traction

Minos E. Beniakar, Panagiotis E. Kakosimos and Antonios G. Kladas

National Technical University of Athens, School of Electrical and Computer Engineering,
9 Iroon Polytechneiou str., 15780 Zografou, Athens, Greece

Design optimization, favoring efficiency maximization, is the subject of extended current research in small electric traction motor applications, aiming the increase in efficiency to be achieved without compromising power density. This paper proposes a mixed technique based on a particular multi-objective, population-based optimization methodology, utilizing a Strength Pareto Evolutionary Algorithm (SPEA) variant combined with the finite element method and analytical tools. The resultant motor design has been validated through measurements on a prototype in-wheel PM motor for a light electric vehicle.

***Index Terms*—Design optimization, strength Pareto evolutionary algorithm, permanent magnet motors, finite element method, electric vehicles.**

I. Introduction

Permanent magnet in-wheel motors have been widely used in electric traction applications due to their inherent advantages of high performance and power density. The nature of the application specifications, regarding both performance and efficiency, in conjunction with the needs for high power quality and reduced weight, have highlighted the necessity for the thorough investigation of their operational characteristics and behavior as well as their systematized optimization [1],[2].

In recent bibliography several optimization techniques have been proposed for electric motor applications, emphasizing on multi-objective strategies. In [3] a multi-objective Differential Evolution (DE) technique is employed for the optimization of a PM actuator, while in [4] a multi-objective approach combining DE with concepts from Strength Pareto Evolutionary Algorithm (SPEA) is applied to an electromagnetic optimization problem. In [5], [6] a modified imperialist competitive algorithm and a bat-inspired optimization methodology, respectively, are employed for the optimization of a brushless DC wheel motor system. In [7] PM motors with soft composite cores are optimized using NSGA 2, while in [8] a particle swarm optimization technique is utilized to increase the efficiency of the powertrain system of a hybrid electric vehicle. Finally, in [9] a multi-objective evolutionary optimization methodology, employing a mesh refinement technique is presented.

In this paper a complete design methodology for an in-wheel Surface Mounted Permanent Magnet (SMPM) motor with Fractional Slot Concentrated Winding (FSCW) and unequal teeth distribution applicable to light electric vehicles is introduced. In the process of assessing motor thermal robustness, a thermal finite element model is used. For the estimation of the PM eddy losses an analytical model is implemented, employing a space harmonic approach based on the representation of the stator armature by an equivalent current sheet disposed over the slot opening.

II. Methodology

Initially, an estimation of the motor structure is achieved by considering classical machine design analytical techniques, according to specifications and space limitations that are mainly dictated by the in-wheel nature of the motor. On a second step, a hybrid SPEA technique, combining features of SPEA and DE, is utilized to optimize the motor geometry on a systematized basis. The improved fitness assignment scheme and the nearest neighbor density estimation method of SPEA 2 are utilized in the algorithm. The raw fitness of every individual is calculated as:

$$R(i) = \sum_{j \in (P^0 + P),\, j \succ i} S(j) \tag{1}$$

where P^0 is the current archive population, P is the current generation population and the symbol $\succ$ corresponds to the Pareto dominance relation. The raw fitness is determined by the strengths of the dominators of a solution both in the Pareto front and the population. The density value assigned to every population member, to discriminate between individuals with identical fitness values, is estimated using the k-*th* nearest neighbor method as:

$$D(i) = \frac{1}{\sigma_i^k + 2} \tag{2}$$

where σ_i^k is the distance of the i-*th* population member to the k-*th* nearest neighbor. The overall fitness value of an individual is calculated as:

$$F(i) = R(i) + D(i) \tag{3}$$

However, the archive truncation method of SPEA 2 has been replaced by the clustering analysis technique of SPEA 1. The preservation of boundary solutions is less critical in such applications where the preliminary design procedure delivers a set of design variables adequately close to the optimum front, contrary to the need for computationally efficient reduction of the archive size.

Additionally, the concept of differential vectors used in DE is employed during the tournament selection to increase trial vector diversity over the mating pool space. In the process of donor formulation, mutation and crossover, the standard DE processes are employed [3]. The mutation factor is set equal to F=0.85 and the crossover probability equal to F_{CR}=0.8. Forced mutation is used for at least one design variable of every trial

DOI: 10.1109/TMAG.2014.2347963

vector in order to avoid vector duplication. An additional promotion probability F_{PND}=0.5, that randomly promotes the trial or the current population member to the next generation, if neither dominates, is used. The DE strategy employed is the DE/local-to-best/1/bin, where the best so far vector is a randomly selected member of the Pareto front. For every trial vector two difference vectors are utilized as follows:

$$v_{i,G} = x_{i,G} + F\left(x_{best,G} - x_{i,G}\right) + F\left(x_{r2,G} - x_{r3,G}\right) \quad (4)$$

The constraints handling strategy is the "death penalty". For every trial vector generated in each generation, constraint functions are evaluated and the potential population member is immediately rejected if at least a single constraint is violated. The main problem constraints are the satisfaction of the motor's minimum torque capacity for nominal and overload conditions and its thermal robustness. For the two aforementioned operating states, the electromagnetic torque versus power angle characteristics are constructed through a series of FE analyses and the torque capacity of the respective geometry for overload and nominal load is calculated. Additionally, a thermal FE model considering the overload condition is used to evaluate the maximum temperature values in the motor magnets and windings.

The boundary constraints, regarding the motor's geometric parameter values, are handled using the bounce-back method. If a trial vector exceeds any of the prescribed bounds, it is replaced by a valid one that satisfies all boundary constraints.

The block diagram of the overall optimization procedure is illustrated in Fig. 1.

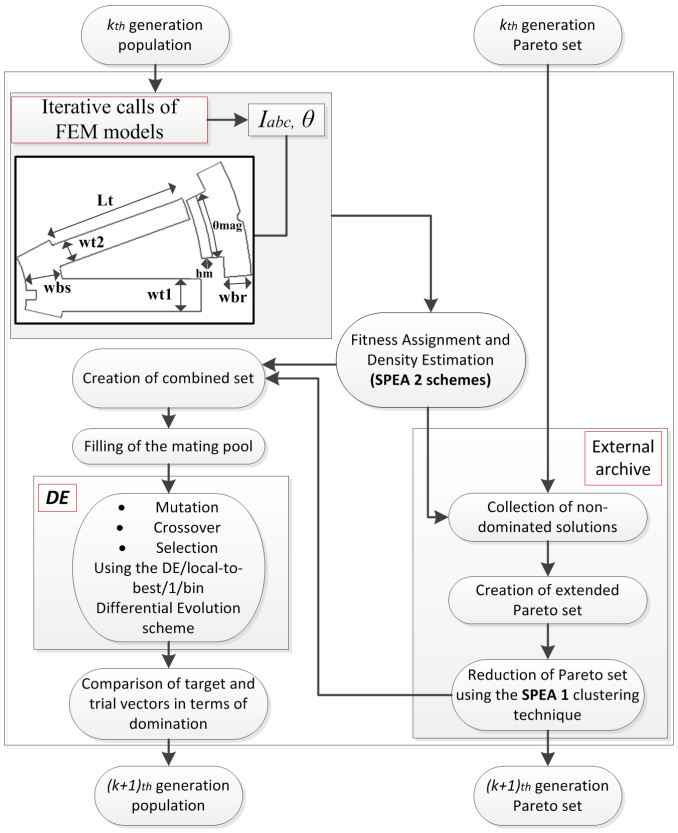

Fig. 1. Optimization procedure main flowchart.

The selected design vector comprises seven key design parameters and the optimization profile accounts for performance, efficiency and power quality. The selected design variable vector is:

$$X_G = \left[k_{un} \quad \theta_{mag} \quad L_t \quad W_{t1} \quad h_{mag} \quad w_{bs} \quad w_{bi}\right]_G \quad (5)$$

where k_{un} is the unequality ratio, θ_{mag} is the magnet angle, L_t is the stator tooth length, W_{t1} is the width of stator thicker tooth, h_{mag} is the magnet height, w_{bs} is the stator back iron thickness and w_{br} is the rotor back iron thickness.

The three objective functions F_1, F_2, F_3 correspond to maximization of torque capability, minimization of total iron, PM eddy and copper losses and minimization of back-EMF harmonic content and torque ripple, respectively. This objective profile accounts for performance, efficiency and power quality. The objective functions are expressed as follows:

$$F = \left[F_1 \quad F_2 \quad F_3\right] = \left[\frac{T_{m,0}}{T_m} \quad \frac{P_{loss}}{P_{loss,0}} \quad \left(0.5 \cdot \frac{THD_{EMF}}{\left(THD_{EMF}\right)_0} + 0.5 \cdot \frac{T_r}{T_{r,0}}\right)\right] \quad (6)$$

where the index *0* refers to the electromagnetic characteristics of the initial design.

Figure 2(a) shows the parameterized motor geometry and the main design variables. Figures 2(b) and 2(c) depict the concepts of (a) differential vectors and (b) bounce-back boundary constraints handling, utilized in the DE algorithm.

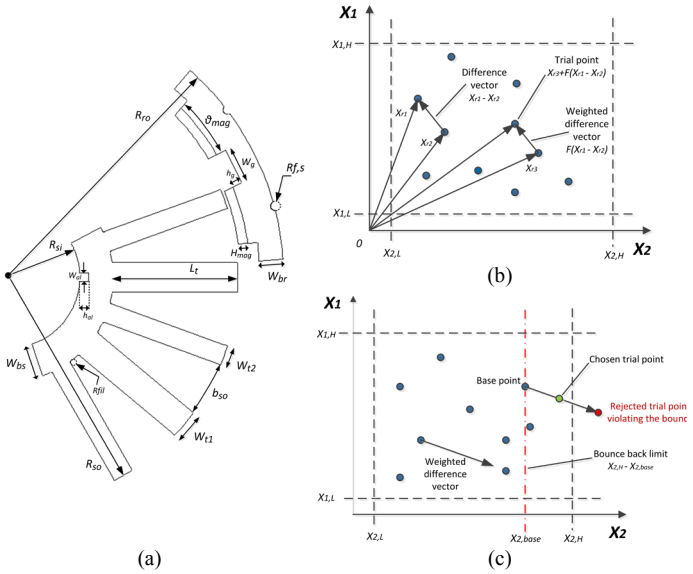

Fig. 2. Motor geometry parameterization and visualization of (b) the differential vectors and (c) the bounce back constraint handling techniques.

Thermal robustness, overall weight and manufacturing complexity are also considered in the optimization process, either via appropriate constraints or through á posteriori data filtering.

Manufacturing complexity has been addressed by taking into account the relative slot dimensions and shape, using empirical analytical expressions [3]. In particular, two main issues where considered: the maximization of the slot fill factor and consequently the maximization of the wire diameter to increase efficiency and the utilization of pre-shaped coils through the adoption of an open-slot configuration.

DOI: 10.1109/TMAG.2014.2347963

The unequal teeth distribution provides an easier to manufacture structure, while increasing the resulting coil pitch. The open slot configuration allows for better control of the coils production process, increasing the fill factor value and allowing for the use of pre-shaped coils, reducing manufacturing cost and complexity. Additionally, due to flexible nature of the copper material the end winding handling is easier, and for high fill factor values wire damage is prevented.

To enable the precise calculation of the temperature distribution in the motor magnets, an analytical model is used to estimate the respective eddy-current losses on the PMs, considering the winding configuration, the basic motor dimensions and the calculated input current of the motors. In particular, a model that considers both space and time harmonics has been implemented based on [10],[11]. The analytical model is based on the representation of the stator ampere-turns distribution by an equivalent current sheet of infinitesimal thickness disposed over the slot opening. For the needs of the analysis, only the fundamental of the line current, as calculated from the FE model, was taken into account, as the current harmonics were unknown.

For alternate teeth wound motor configurations the equivalent current density that accounts for the armature reaction is expressed as:

$$J_s(\theta_r, R_s, t) = \sum_u^{\infty}\sum_v^{\infty} \mp \frac{2N_{ph}I_u}{\pi R_s} K_{wn}K_{sov} \cos\left[(up_r \pm vp_s)\omega_r t \pm vp_s\theta_r + \theta_u\right] \quad (7)$$

where R_s is the stator outer radius, I_u is the amplitude of the harmonic phase current, N_{ph} is the number of series turns per phase, p_r is the number of rotor pole pairs, p_s is the number of equivalent stator pole pairs, ω_r is the motor rotational speed, u is the order of the space harmonic, v is the order of the phase current time harmonic, θ_u is the phase current harmonic angle and K_{sov} is the slot opening factor. The winding factor K_{wn} is set equal to 1 for all harmonic orders due to the unequal teeth distribution.

For an in-wheel motor, with external rotor configuration, the resulting eddy-current losses in the surface mounted PMs are calculated as:

$$P_{ed} = 2p_r \frac{\omega_r}{2\pi} \int_0^{2\pi/\omega_r} \int_{R_m}^{R_r} \int_{-\alpha/2}^{\alpha/2} \rho J_m^2 r dr d\theta_r dt = \sum_u \sum_v \left(P_{cuv} + P_{auv}\right) \quad (8)$$

where R_m is the inner magnet radius, R_r is the inner rotor radius, J_m is the induced eddy current in the PMs and α is the pole pitch arc. The loss terms P_{auv} and P_{cuv} are analyzed in [12],[13]. Figure 3 illustrates the winding configuration for the motor and the respective qualitative electric loading distribution that accounts for the produced MMF waveform and the results of the analytical model, regarding the magnetic field distribution and the variation of the PM eddy losses.

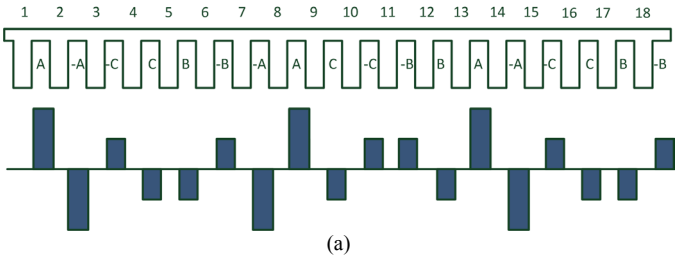

(a)

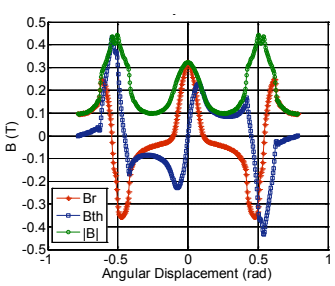

(b)

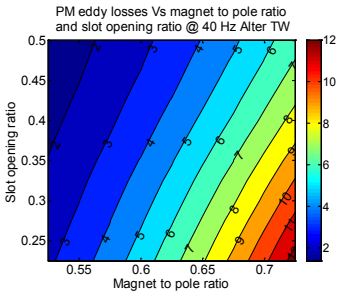

(c)

Fig. 3. (a) Electric loading of the motor having a 18 slot single layer concentrated winding configuration, (b) Components of the magnetic field due to the armature reaction of the motor and (c) Variation of the PM eddy losses as a function of the slot opening and the magnet to pole ratio, calculated with the analytical model.

The thermal robustness of every motor candidate design is considered through a 2D thermal FE model. For every generation member after the solution of the magnetic FE model and the analytical PM eddy losses model, the respectively cooper, iron and magnet eddy losses are imputed into the thermal model and the temperature distribution is evaluated.

The relatively small size of the rotor, causing a limited dissipation surface, along with its high power density can incur a significant temperature rise during overload operation, compromising the performance of the motor due to magnets thermal demagnetization [12],[13]. The introduction of the aforementioned thermal constraints in the optimization routine renders the preservation of temperature rise within prescribed borders.

III. Results and Discussion

The optimization procedure yielded a set of Pareto optimal solutions set. The final geometry is selected as a tradeoff between weight minimization and efficiency maximization. The resulting Pareto front in the 3D objective function space is presented in Fig. 4.

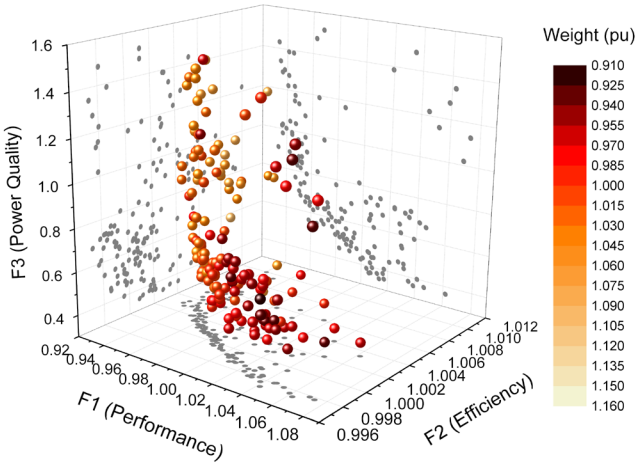

Fig. 4. Optimization results: final Pareto front

Figure 4 also depicts the three projections of the Pareto front on the respective objective function surfaces. The overall motor weight is considered in the optimization procedure as a selection criterion between the Pareto front members. The weight variation of the resulting optimum motors is also

DOI: 10.1109/TMAG.2014.2347963

depicted in Fig. 4, using a color map. The conflicting nature of the objective functions is evident from the final shape of the front [3-5],[8-9]. The design parameters values for the final selected motor are tabulated in Table I.

For the final geometry a 3D thermal model was utilized to validate the results of the respective 2D model. The constructed housing of the motor is also modeled. The temperature distribution in the motor parts, in extracted view, is illustrated in Fig. 5.

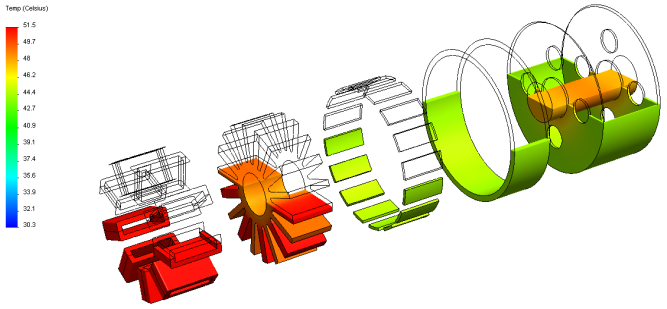

Fig. 5. Results of the 3D thermal model, Temperature distribution for overload operation

TABLE I
DESIGN CHARACTERISTICS OF THE FINAL MOTOR

Design variables	Magnet angle (%)	60
	Tooth width (mm)	7.00
	Back iron stator thickness (mm)	8.00
	Back iron rotor thickness (mm)	6.00
	Unequality ratio (%)	0.7
	Copper Fill factor	0.5
	Total mass (kg)	2.95

The manufactured in-wheel SMPM motor has been tested for various operating conditions validating the accuracy of the proposed design methodology. Figure 6 shows (a) the stator and winding configuration of the manufactured prototype and (b),(c) the prototype motor mounted on the chassis of the electric vehicle. Figure 7 depicts the measured phase voltage and electromagnetic torque Vs current characteristics.

(a) (b) (c)

Fig. 6. (a) Stator and winding of the prototype motor (b),(c) Manufactured prototype mounted on the electric vehicle chassis.

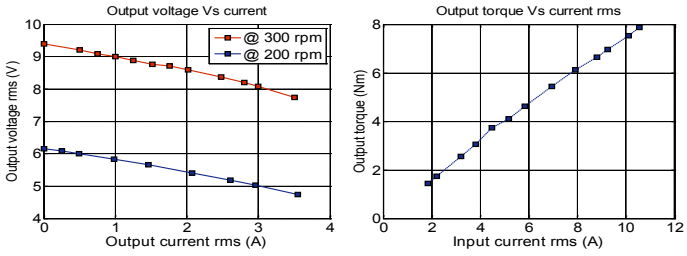

(a) (b)

Fig. 7. Experimental results, (a) phase voltage Vs current and (b) electromagnetic torque Vs current measurements.

IV. CONCLUSION

An evolutionary, population-based optimization methodology has been introduced and implemented in the design of an in-wheel PM motor, with unequal stator teeth distribution and fractional slot concentrated winding configuration, for a light electric vehicle. A SPEA 2 based optimization algorithm that utilizes the concept of differential vectors in the tournament selection and the clustering technique of SPEA 1 is developed. In the optimization routine both electromagnetic and thermal FE models and analytical solutions for the magnet eddy losses are integrated. Thermal robustness, manufacturing complexity and motor overall weight are also assessed. The optimization results are validated by measurements on a manufactured prototype in-wheel motor, mounted on an electric vehicle.

ACKNOWLEDGMENT

The research leading to these results has received funding from the EU and General Secretariat of Research and Technology of Greece under 09SYN-51-988 Grant.

REFERENCES

[1] Jiabin Wang; V.I. Patel and Weiya Wang, "Fractional-Slot Permanent Magnet Brushless Machines with Low Space Harmonic Contents," *IEEE Trans. Magn.*, vol.50, no.1, pp.1-9, Jan. 2014.

[2] Hafner, Martin; Finken, T.; Felden, M.; Hameyer, K., "Automated Virtual Prototyping of Permanent Magnet Synchronous Machines for HEVs," *IEEE Trans. Magn*, vol.47, no.5, pp.1018-1021, May 2011.

[3] M.E. Beniakar, A.G. Sarigiannidis, P.E. Kakosimos and A.G. Kladas, "Multi-objective Evolutionary Optimization of a Surface Mounted PM Actuator with Fractional Slot Winding for Aerospace Applications," *IEEE Trans. Magn.,* vol.50, no.2, pp. 665-668, Feb. 2014.

[4] G. Caravaggi Tenaglia and L. Lebensztajn, "A Multiobjective Approach of Differential Evolution Optimization Applied to Electromagnetic Problems," *IEEE Trans. Magn.*, vol.50, no.2, pp.625-628, Feb. 2014.

[5] L.D.S. Coelho, L.D. Afonso and P. Alotto, "A Modified Imperialist Competitive Algorithm for Optimization in Electromagnetics," *IEEE Trans. Magn.*, vol.48, no.2, pp.579-582, Feb. 2012.

[6] T.C. Bora, L.D.S. Coelho and L. Lebensztajn, "Bat-Inspired Optimization Approach for the Brushless DC Wheel Motor Problem," *IEEE Trans. Magn.*, vol.48, no.2, pp.947-950, Feb. 2012.

[7] Gang Lei, Jianguo Zhu, Youguang Guo, Keran Shao and Wei Xu, "Multiobjective Sequential Design Optimization of PM-SMC Motors for Six Sigma Quality Manufacturing," *IEEE Trans. Magn.*, vol.50, no.2, pp.717-720, Feb. 2014.

[8] Al-Aawar, N.; Hijazi, T. M.; Arkadan, A.A., "Particle Swarm Optimization of Coupled Electromechanical Systems," *IEEE Trans. Magn*, vol.47, no.5, pp.1314-1317, May 2011.

[9] Di Barba, P., "Evolutionary Multiobjective Optimization Methods for the Shape Design of Industrial Electromagnetic Devices," *IEEE Trans. Magn*, vol.45, no.3, pp.1436-1441, March 2009.

[10] Yunkai Huang, Jianning Dong, Long Jin, Jianguo Zhu and Youguang Guo, "Eddy-Current Loss Prediction in the Rotor Magnets of a Permanent Magnet Synchronous Generator With Modular Winding Feeding a Rectifier Load," *IEEE Trans. Magn.*, vol.47, no.10, pp.4203-4206, Oct. 2011.

[11] D. Ishak, Z.Q. Zhu and D. Howe, "Eddy-current loss in the rotor magnets of permanent-magnet brushless machines having a fractional number of slots per pole," *IEEE Trans. Magn.*, vol.41, no.9, pp.2462-2469, Sept. 2005.

[12] S. Ruoho, J. Kolehmainen, J. Ikaheimo and A. Arkkio, "Interdependence of Demagnetization, Loading, and Temperature Rise in a Permanent-Magnet Synchronous Motor," *IEEE Trans. Magn.*, vol.46, no.3, pp.949-953, March 2010.

[13] Jianning Dong, Yunkai Huang, Long Jin, Heyun Lin and Hui Yang, "Thermal Optimization of a High-Speed Permanent Magnet Motor," *IEEE Trans. Magn.*, vol.50, no.2, pp.749-752, Feb. 2014.